Strain and deformation history in a syntectonic pluton. The case of the Roses granodiorite (Cap de Creus, Eastern Pyrenees)

J. CARRERAS, E. DRUGUET, A. GRIERA & J. SOLDEVILA
Departament de Geologia, Universitat Autònoma de Barcelona, 08193 Bellaterra, Barcelona, Spain (e-mail: jordi.carreras@uab.es)

Abstract: The Roses granodiorite is a Variscan stock with well developed syn- and post-magmatic deformation structures that crops out in the Pyrenean Axial Zone. Analysis of structures reveals a continuous deformation history during and after magma cooling. The deformation history is divided on the basis of mechanical behaviour into two stages: an early one with the development of magmatic structures and a late stage with the development of mylonitic fabrics along shear zones. Both stages are separated in time by the emplacement of aplite-pegmatite dykes. Time of dyke emplacement is thought to coincide with a sudden change in rheology of the granodiorite. The abundance of quartz dioritic enclaves permits the use of shape analysis to characterize the magmatic fabric as a homogeneous deformation. Later solid-state deformation led to the development of an inhomogeneous deformation pattern with different sizes of anastomosing shear zones wrapping around lozenge-shaped domains. The displacement/width ratio measured in shear zones ranges between one and two orders of magnitude. The Roses granodiorite is thought to be a synkinematically emplaced stock which records a continuous deformational history with two distinct deformation stages, both recording bulk finite strains of similar order of magnitude but with a marked difference in finite strain distribution.

Granitoid batholiths and stocks are abundant in the Variscan basement of the Pyrenees (Fig. 1). Although these were initially referred to in the literature as Variscan late-tectonic intrusions (e.g. Maladeta Massif; Zwart 1979), more recent studies have revealed the syntectonic nature of many of these plutons (e.g. Bassiès Granite, Gleizes *et al.* 1991). Such studies have been carried out both on the internal fabrics, by the use of the AMS method (Leblanc *et al.* 1996; Gleizes *et al.* 1998*a*), and on the structures present in the country rock aureoles (Evans *et al.* 1998). Thus, most Variscan plutons in the Pyrenees are now well characterized by means of deformational features and relative time of intrusion, being generally accepted as emplaced during a main Variscan deformational event. Furthermore, some of these syntectonic plutons are also affected by shear belts developing mylonite bands (Fig. 1). The age and geotectonic significance of the mylonite belts is still under debate (Guitard 1970; Carreras *et al.* 1980; Lamouroux *et al.* 1980; Saillant 1982; Delaperrière *et al.* 1994).

The Roses and Rodes massifs are two synkinematically emplaced stocks of mainly granodioritic composition, located on the Cap de Creus Peninsula, which forms the easternmost outcrop of the Palaeozoic basement in the Pyrenean Axial Zone (Fig. 1). The Roses stock, elongated in a NW–SE direction, was emplaced into low grade Cambro-Ordovician metasediments, developing a narrow contact aureole of spotted phyllites and hornfelses. The enclosing metasediments exhibit a polyphase history with two main deformation events. The first is responsible for a layer-subparallel penetrative cleavage referred to as the regional foliation. The second is represented by an inhomogeneously distributed crenulation cleavage which postdates the contact metamorphism. This deformation history is revealed by contact metamorphic porphyroblasts that grew over the main foliation, but show a crenulation cleavage related to the late folding phase wrapping around them.

The emplacement of the Roses granodiorite started before the late folding phase. Folds related to the crenulation in the enclosing metasediments were contemporaneous with shear zone development in the granodiorite (Carreras & Losantos 1982). These two distinct types of structures, folds in the metasediments and shear zones in the granodiorite, possibly reflect how the two lithological units with different rheological properties responded to deformation.

The orientation of all Variscan structures in the Roses granodiorite is affected by a local Alpine overturning. This overturning occurs all along the southern border of the Pyrenean Axial Zone (Vergely 1970; Muñoz *et al.* 1986) and

From: ALSOP, G. I., HOLDSWORTH, R. E., MCCAFFREY, K. J. W. & HAND, M. (eds) 2004. *Flow Processes in Faults and Shear Zones*. Geological Society, London, Special Publications, **224**, 307–319. 0305-8719/$15.00

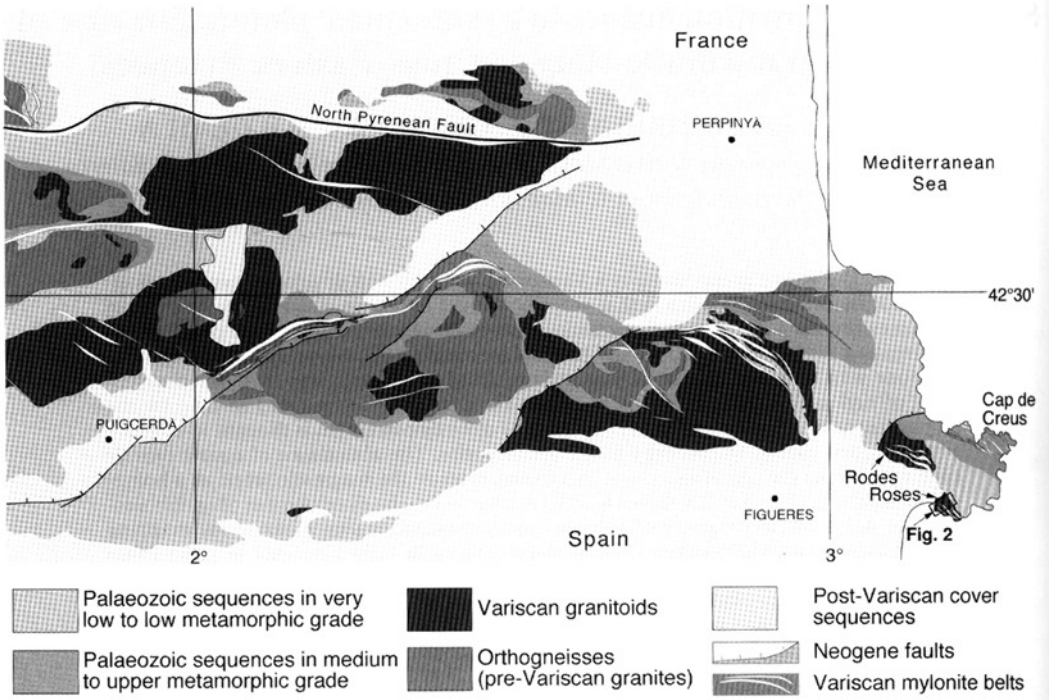

Fig. 1. Sketch of the main lithological units and structures in the Variscan of the eastern Pyrenees and location of the Roses granodiorite.

causes originally NE-dipping dextral shear zones to appear as sinistral ones (Carreras 2001).

Progressive development of structures in the Roses granodiorite

Like some other Variscan granitoid massifs of the Pyrenean basement (e.g. Querigut Massif; Marre 1973 and Bassiès granodiorite; Gleizes *et al.* 1991), the Roses granodiorite shows an early homogeneous magmatic fabric and a network of low-temperature shear zones (Fig. 2) that gave rise to inhomogeneous mylonitization at low greenschist facies, presumably of Variscan age (Carreras & Losantos 1982). This was followed by late cataclasis developed in narrow bands of millimetre thickness (Simpson *et al.* 1982). A range of magmatic-state/pre-full crystallization to solid-state/crystal plastic strain fabrics developed throughout the cooling history from high-temperature to the low-temperature regimes, in a manner similar to that proposed by Gapais (1989) in a general model.

The existence of this continuous gradation of structures and the difficulty in establishing a clear distinction between the early synmagmatic structures and the fabrics related to the late shear zones will be discussed below. This will be followed by an analysis of the magmatic fabrics and the structures related to late solid-state shearing. For the sake of simplicity and objectivity, these analyses will be presented separately, using the presence of a swarm of aplite-pegmatite dykes to distinguish between the early structures predating dyke emplacement and those affecting the dykes (Fig. 3).

Magmatic fabric and enclaves

The oldest tectonic structure in the granodiorite is a pre-full crystallization fabric (Hutton 1988) or magmatic fabric (Paterson *et al.* 1989), defined by a preferred orientation of subhedral feldspar, sometimes with tiling between pairs of crystals, along with a weaker alignment of mafic minerals (biotite and amphibole). Additional evidence of magmatic flow is the preferred orientation of elongated enclaves (Fig. 4a) and the presence of schlieren layering in the granodiorite. These are all indicative of synmagmatic deformation.

Synmagmatic foliations trend E–W to NW–SE (Figs 3 & 5) in a vaguely curved disposition. The magmatic fabric postdates the regional foliation in the enclosing sediments as is

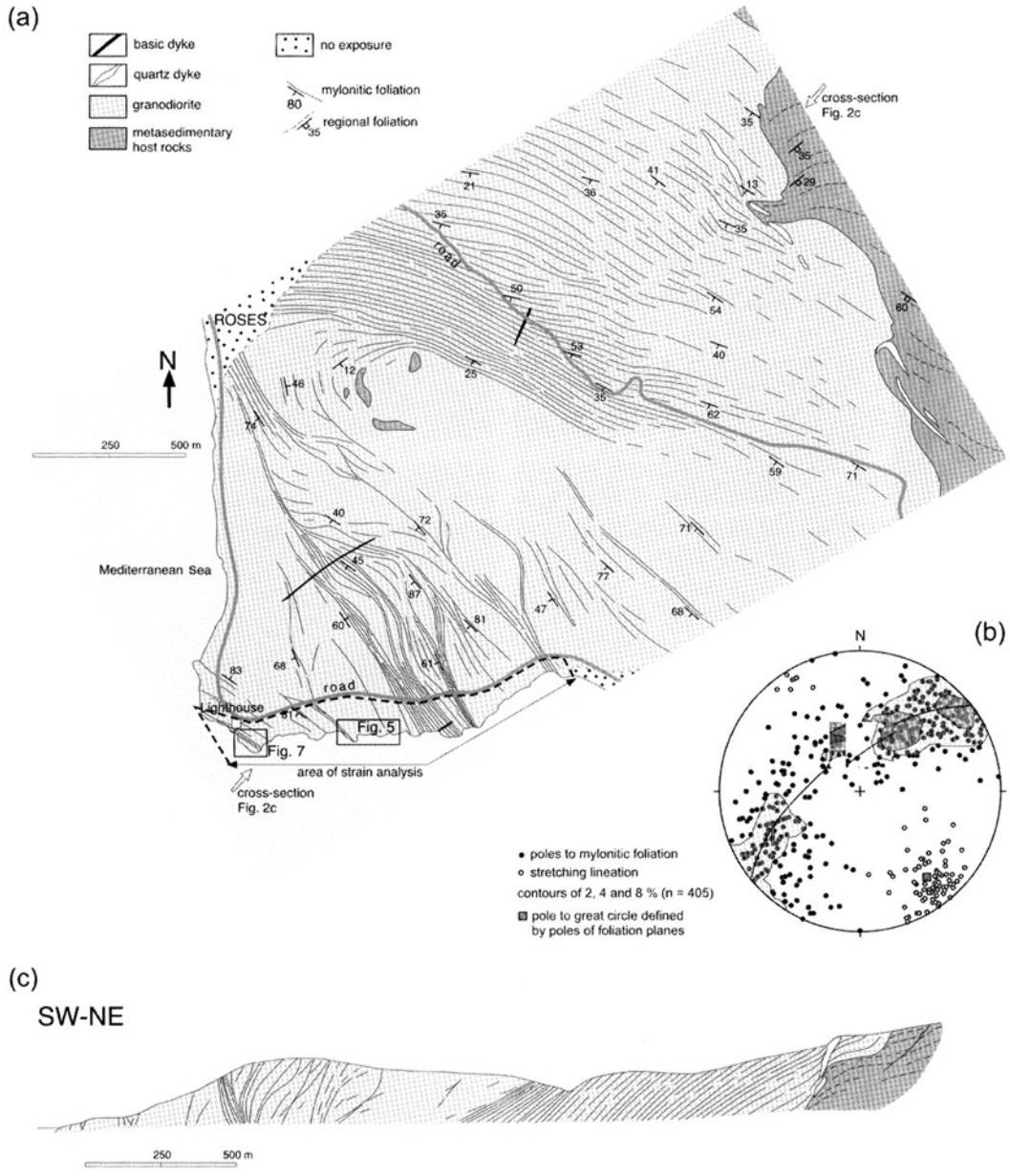

Fig. 2. Geological setting of the Roses granodiorite and the studied area. (**a**) Structural map of the studied area showing traces of the main shear zones. Location of the area is shown in Fig. 1. (**b**) Stereoplot showing the orientation of the poles to the mylonite foliation and the associated stretching lineation. (**c**) Section across the Roses granodiorite.

evidenced from the presence of foliated metasedimentary xenoliths in the granodiorite.

The Roses granodiorite is characterized by an abundance of enclaves (Figs 4a, b, c, & 5), most of them microquartz dioritic, with abundant mafic minerals (biotite and amphibole). There is also a small proportion of metasedimentary xenoliths. Enclave distribution is inhomogeneous, with the presence of some dismembered synplutonic microquartz dioritic sheets. The enclaves are predominantly flattened and show a marked preferred orientation subparallel to the magmatic foliation (Fig. 4a, c). This foliation exhibits little or no deflection around

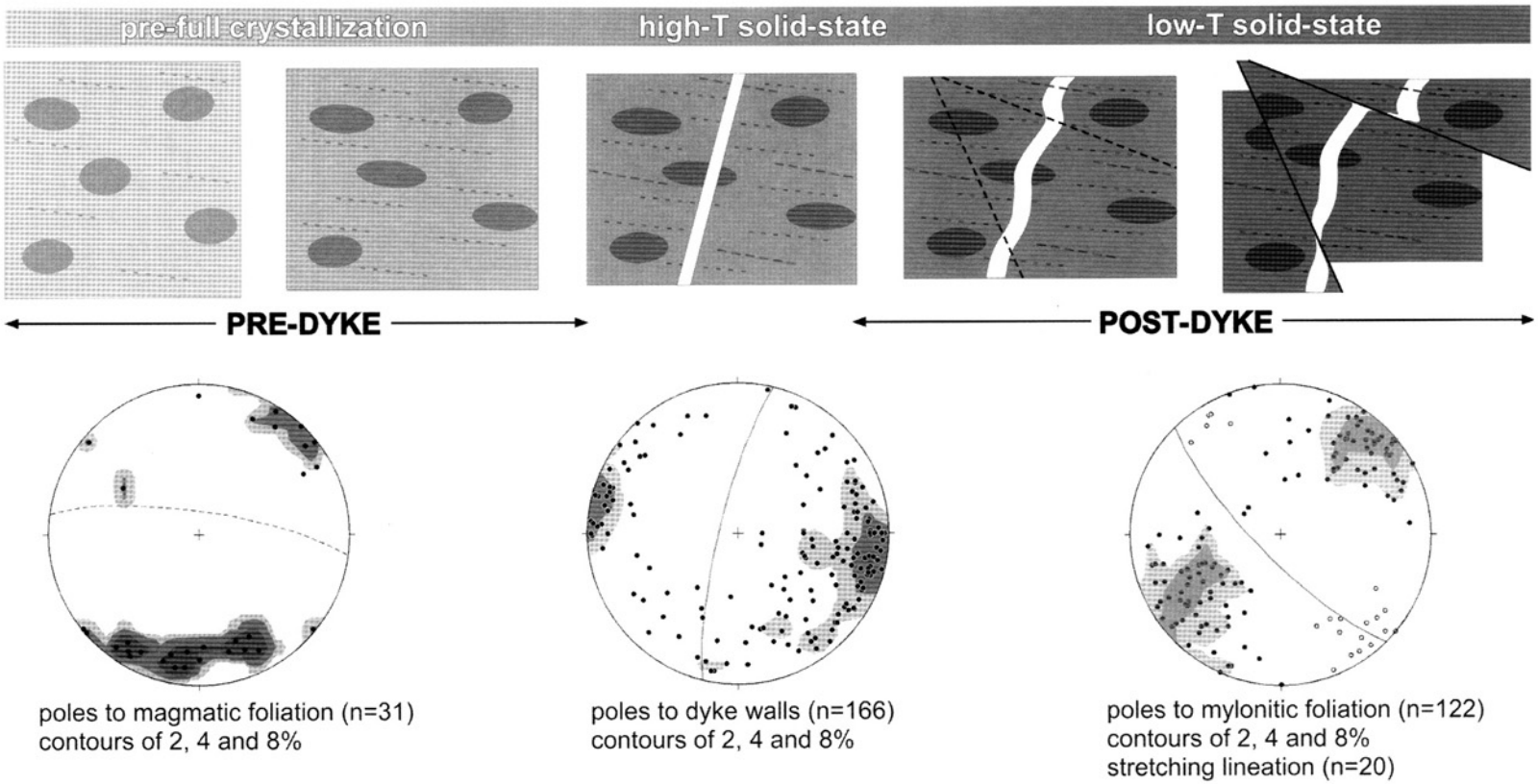

Fig. 3. Schematic qualitative model of the structural history of Roses granodiorite. The progressive development of structures from high to low temperature can be divided in two major stages with regard to the time of dyke emplacement. Stereoplots of orientation of different structures are also shown.

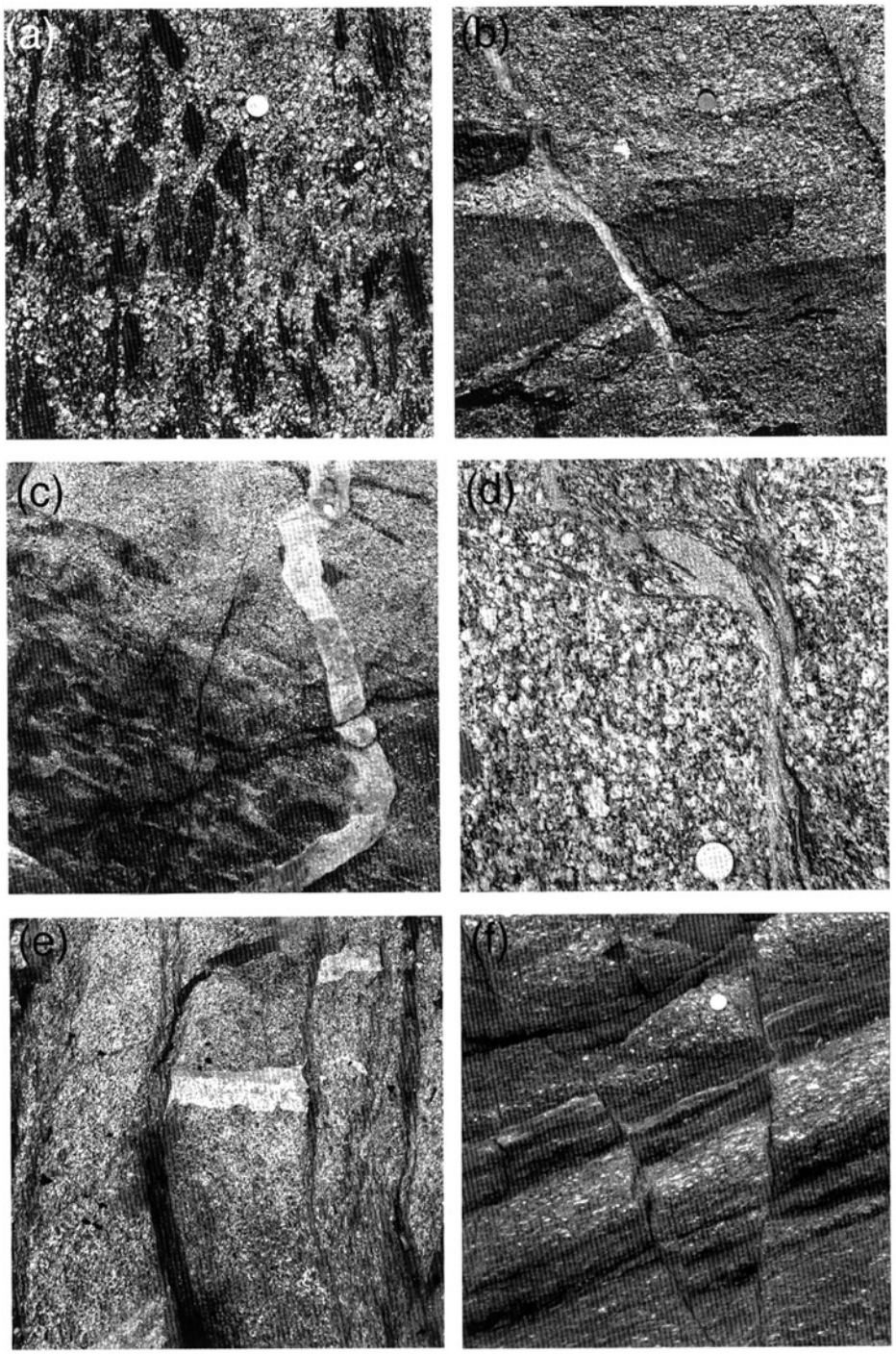

Fig. 4. Mesoscopic scale structures in the Roses granodiorite. (**a**) Preferred orientation of elongate microquartz dioritic enclaves of a former synmagmatic dyke. (**b**) Straight aplite vein cutting across the magmatic fabric marked by orientation of enclaves. (**c**) Syntectonically emplaced leucocratic dyke forming open folds with axial planes parallel to the magmatic fabric. (**d**) Microgranite with igneous texture emplaced along a curved shear zone. (**e**) Leucocratic dyke of aplite in the granodiorite cut by sinistral shear zones (**f**) Brittle–ductile transition conjugate fractures cutting across mylonites.

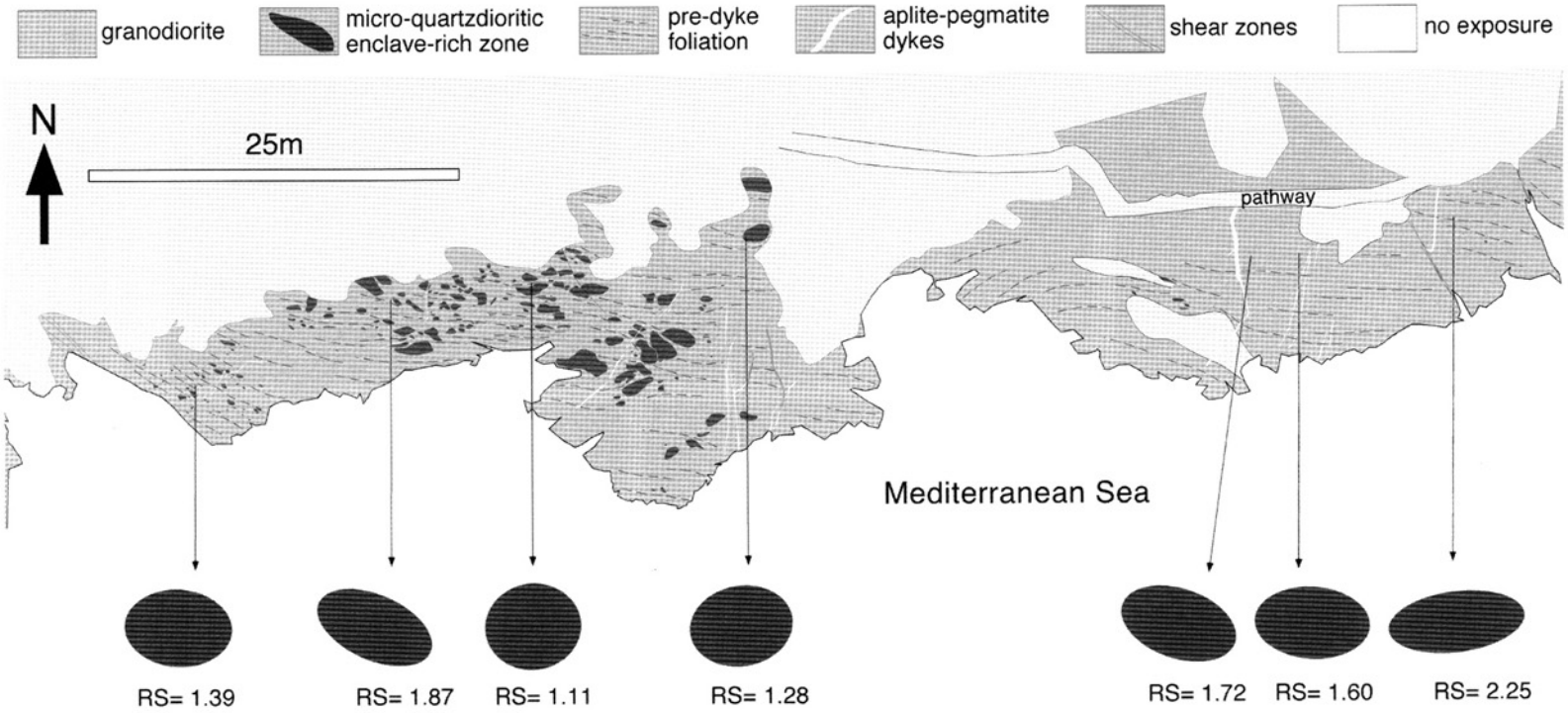

Fig. 5. Pre-dyke finite strains obtained from two-dimensional analysis of enclave shapes in sections close to the *XZ* plane, in a domain without significant late shearing. For each locality, the mean strain axial ratio (RS) is shown with an ellipse showing mean orientation and shape of the strain ellipse. Location is shown in Fig. 2.

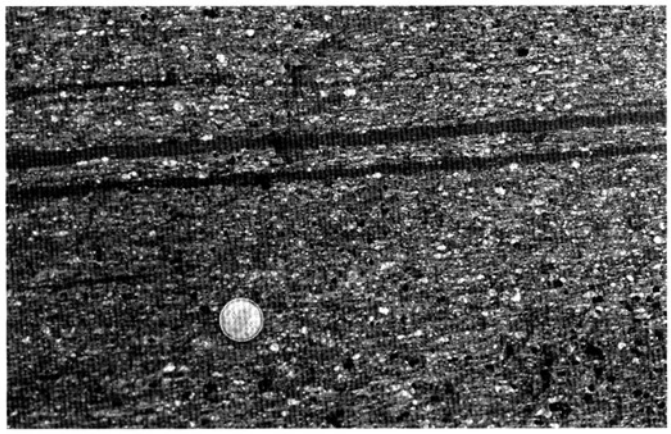

Fig. 6. Part of an extremely elongated enclave of quartz diorite with an axial ratio of about 150:1 from the inner part of a shear zone.

elongated enclaves, from which it is envisaged that the enclaves were slightly more competent during development of the magmatic fabric (Gay 1968; Paterson & Miller 1998). Later solid-state deformation would probably have caused a further decrease in viscosity ratio, in agreement with the work by Tobisch & Williams (1998).

Leucocratic dykes

In most domains the magmatic fabric is cut by straight granophyric aplite-pegmatite veins and dykes (Fig. 4b) that vary in size from a few millimetres to about one metre in width and tens of metres in length. They form a swarm of dykes of predominant NNE–SSW original orientation (Fig. 3), cross-cutting the magmatic fabric and the elongated enclaves at a high angle (70–90°). Thus, dykes are presumed to occur in tension fractures related to the same stress/strain field that produced the magmatic foliation. Furthermore, the dykes are slightly folded locally, with fold axial planes parallel to the earlier magmatic fabric (Fig. 4c), suggesting that high-temperature solid-state deformation occurred with a similar orientation in the granodiorite during and after dyke emplacement. Dykes do not show significant refraction when passing through host/enclave interfaces (Fig. 4b). The emplacement of dykes into a network of brittle fractures affecting the granodiorite is presumed to have been coeval with a sudden change in rheology of the granodiorite stock. The granodiorite, at a submagmatic stage with an overpressured residual leucogranitic melt, would have experienced a 'melt-enhanced embrittlement' (Hollister & Crawford 1986; Davidson *et al.* 1994; Brown & Solar 1998; Handy *et al.* 2001).

Shear zones and associated mylonites

Post-dyke deformation is mainly related to the development of shear zones, affecting both granodiorites and leucocratic dykes (Figs 4e & 6). In their present orientations shear zones form a NW–SE anastomosing network with predominant steep dips (Figs 2 & 3) and dominantly sinistral strike–slip components. Associated mylonite bands range in thickness from a few millimetres to more than 500 m. In contrast with magmatic structures, which are widely distributed in the entire stock, the shear zones represent a highly inhomogeneous deformation leaving different-sized elongate domains nearly untouched by mylonitization (Simpson *et al.* 1982). Movement direction is shown by the disposition of the stretching lineation (Figs 2b & 3). The sense of movement can be depicted easily from the marginal obliquity of the mylonitic foliation and the offset of aplitic dykes in appropiate sections (Fig. 4e). In addition there are abundant shear-band structures with dispositions always coherent with the depicted sense of shear.

The anastomosing and fan-like pattern, with dominant sinistral shear zones and less abundant dextral ones, could represent a conjugated system. However, shear directions do not form two maxima but a single one coinciding with the intersection direction of differently orientated planes (Figs 2b & 3). Thus, in a stereoplot, poles of foliation planes define a great circle with its

pole coinciding with the stretching lineation. This geometrical relation appears to be a common feature of shear belts and is analogous to that described by Ramsay and Allison (1979) in the Maggia Nappe.

Most mylonites developed under greenschist facies metamorphic conditions, assisted by strong quartz recrystallization and new growth of chlorite, albite, white mica and epidote. Some broad shear zones contain bands, ranging up to a few metres in width, where the mylonites are completely depleted of quartz, and albite–chlorite mylonites form. This mineralogical and chemical transformation of the mylonites may have occurred along zones where fluid was channelled. These zones are probably related to the intrusion of quartz veins and dykes contemporaneous to mylonitization.

Although nearly all shear zones formed in the solid-state and under greenschist facies conditions, a peculiar type has been observed. This consists of a complex network of centimetre-thick shear zones with fine-grained granitic isotropic material injected along them (Fig. 4d). This particular type of shear zone is considered to represent the earliest stages of localized deformation before the complete crystallization of the granodiorite, and is presented as another argument for the transition from magmatic to solid-state deformation during the cooling of the stock.

Late brittle fractures

At the terminations of shear zones, but also cutting across ductile shear zones (Fig. 4f), very narrow fractures with associated cataclasites are present. Although brittle fractures on shear zone tips occur in association with shear zone propagation (Simpson 1983), the cross-cutting ones represent the latest structures formed in the granodiorite. These fractures commonly form conjugate sets but, in contrast with preceding ductile shear zones, conjugate brittle fractures always occur at an acute angle to the compressional field, with principal compression axis in an orientation close to north–south. Note that the final orientation of the compressional direction is similar and coherent with the orientation required to develop the initial magmatic fabric, direction of dyke emplacement and the later shear zones.

Structure and strain profiles

The abundance of micro-quartzdioritic enclaves permits the use of shape analysis to characterize the magmatic to high-temperature solid-state fabrics and the superimposed effects of later mylonitization developed under greenschist facies conditions. In addition, rotation and thinning of aplite-pegmatite dykes by shearing and related offset enables shear strain determinations across shear zones. Furthermore, the outcrop conditions along the coastal fringe located in Fig. 2a, with abundant sections close to plane view, enable the establishment of strain profiles across the described structures and the determination of the kinematic pattern associated with shearing.

Deformation predating dykes

Strain analysis has been performed using the Rf/ϕ technique (Lisle 1985) for enclave populations in different locations. By measuring shape ratio and orientation of the enclaves one can infer information about the total strain and put some constraints on the deformation history. Previously, mafic enclaves have been used for quantitative estimation of finite strain (Ramsay & Hubber 1983; Hutton 1988; Williams and Tobisch 1994; Tobisch & Williams 1998; Wenk 1998). However, the reliability of enclaves as strain markers has been questioned because of the existence of some variables that cannot be related directly to deformation processes (see discussions in Paterson & Vernon 1995 and Tobisch & Williams 1998). Among these variables the most important are: enclave shapes and orientation may reflect other processes besides deformation during emplacement, such as ascent and chamber boundary processes; and the possible contrast in rheology between enclaves and host rocks.

The prevalent subhorizontal sections were not adequate to perform an exhaustive 3D analysis. Instead, a general qualitative examination of enclave population on the entire enclave-rich area was made first, from which it was established that the XZ section of most enclaves is roughly sub-horizontal. After that, a three-dimensional analysis from three different sections at one location was performed to estimate the orientation and shape of the strain ellipsoid. This gave a flattening strain ellipsoid with Rxz approximately 3, Ryz about 2.5, a gently east-dipping XZ plane of finite strain and east-plunging maximum elongation (X). Then, based on the qualitative assessment and the result from three-dimensional analysis, an extensive two-dimensional strain analysis was carried out on the prevalent sub-horizontal sections, close to the XZ plane. Each location corresponds to a homogeneous domain covering a surface ranging from a few square metres up to

about 100 m^2, where undeformed dykes provide evidence for the absence of post-dyke strains. In each locality, between 40 and 70 enclaves were measured. The metasedimentary xenoliths and the dismembered microquartz dioritic sheets have been excluded from the shape analysis. Enclaves with unusual shapes and orientations with regard to the main distribution have also been excluded, as they can yield erroneous results. Rf/ϕ analyses show a pre-dyke finite strain characterized by axial ratios ranging between 1.1 and 4. Figures 5 and 7 show shapes and orientations of pre-dyke finite strains in two different domains. These finite strains represent the sum of a large magmatic strain and a minor high temperature solid-state deformation.

The results probably underestimate the total pre-dyke strain, due to: (1) the presumed viscosity contrast (albeit low) between enclaves and granodiorite; (2) the analysed section, which is not perfectly parallel to the XZ plane of the finite strain ellipsoid; and (3) the earliest deformation in the magmatic history may not have been, or only slightly recorded by the enclaves (Davidson *et al.* 1994). Not withstanding these problems, the strain measurements using enclave shape give an acceptable estimate of finite strain gradients undergone by the granodioritic stock. Bulk results obtained from different localities indicate that there is a slight inhomogeneity in strain and that this is of low intensity but widespread across the entire stock. Extrapolating the observed mean strain values to the entire pluton, the pre-dyke synmagmatic deformation related to emplacement of the stock represents a bulk horizontal shortening of about 33%.

Deformation postdating dykes

In broad mylonitic bands, strain analysis was performed using enclave shape and orientation (Fig. 7). Enclaves reflect the variable degree of deformation due to the high inhomogeneity of strain distribution. In sections closely parallel to the finite XZ plane, RS values greater than 10 are common, with some enclaves reaching values up to RS = 150 (Fig. 6).

In thin shear zones, the best and most reliable strain profiles (Fig. 8) were obtained by applying the Ramsay & Graham (1970) method for shear strain determination. This technique is based on the combined use of sigmoidal pattern of mylonitic foliation and change in orientations and offsets of dykes, assuming a simple shear model for the shear zones. This assumption is supported by the fact that the shear zones are localized along narrow, discrete bands, with foliation patterns following a profile which is close to the one expected for simple shear.

The shear zone profile analyses (Fig. 8) reveal a high inhomogeneity of strain at different scales. A mean shear strain value from each profile has been calculated by means of the total displacement/total width relationship. Furthermore, an analysis of the displacement/width ratio of shear zones is constant on shear zones of different size and ranges between one and two orders of magnitude (Fig. 9). Although the point distribution in this graph has a similar slope to the plot presented in Mitra (1979), significant differences exist concerning the intersecting point along the displacement axis. In the case of the Roses granodiorite, displacement in each shear zone is generally at least ten times its width, and therefore about one order of magnitude greater than in the relationship shown by Mitra (1979).

Averaging the total displacement/total width relationships obtained from different profiles, and evaluating the total width of shear zones versus the total width of unsheared rocks in the area, a bulk shear strain of 1.4 was estimated. This corresponds to a finite strain axial ratio of 3.3. Extrapolating the shear strain values to the entire stock, by means of the movement along the described network of shear zones, we infer a post-dyke bulk horizontal shortening of about 45%.

Discussion and conclusions

The Roses case study shows that enclaves and shear zone profiles are powerful tools for the comparison of deformation during two stages of the stock history. Although the magmatic fabric is less conspicuous than the mylonitic one, it appears that, considering average values, the magnitude of horizontal shortening accommodated during the early pre-dyke stage is lower but of similar order of magnitude to the shortening accommodated during solid-state mylonitization. If we superpose the post-dyke shortening (45%) on the pre-dyke shortening (33%), the granodiorite recorded a bulk horizontal shortening of about 60%. This value is slightly smaller than expected if the two superposed deformations were coaxial.

These two deformation events developed under different temperature conditions and are clearly separated in time by the emplacement of aplite-pegmatite dykes. However, the presence of high-temperature fabrics related to open folding of synkinematic dykes and the presence of shear zones with igneous material injected along them, indicate the continuity of

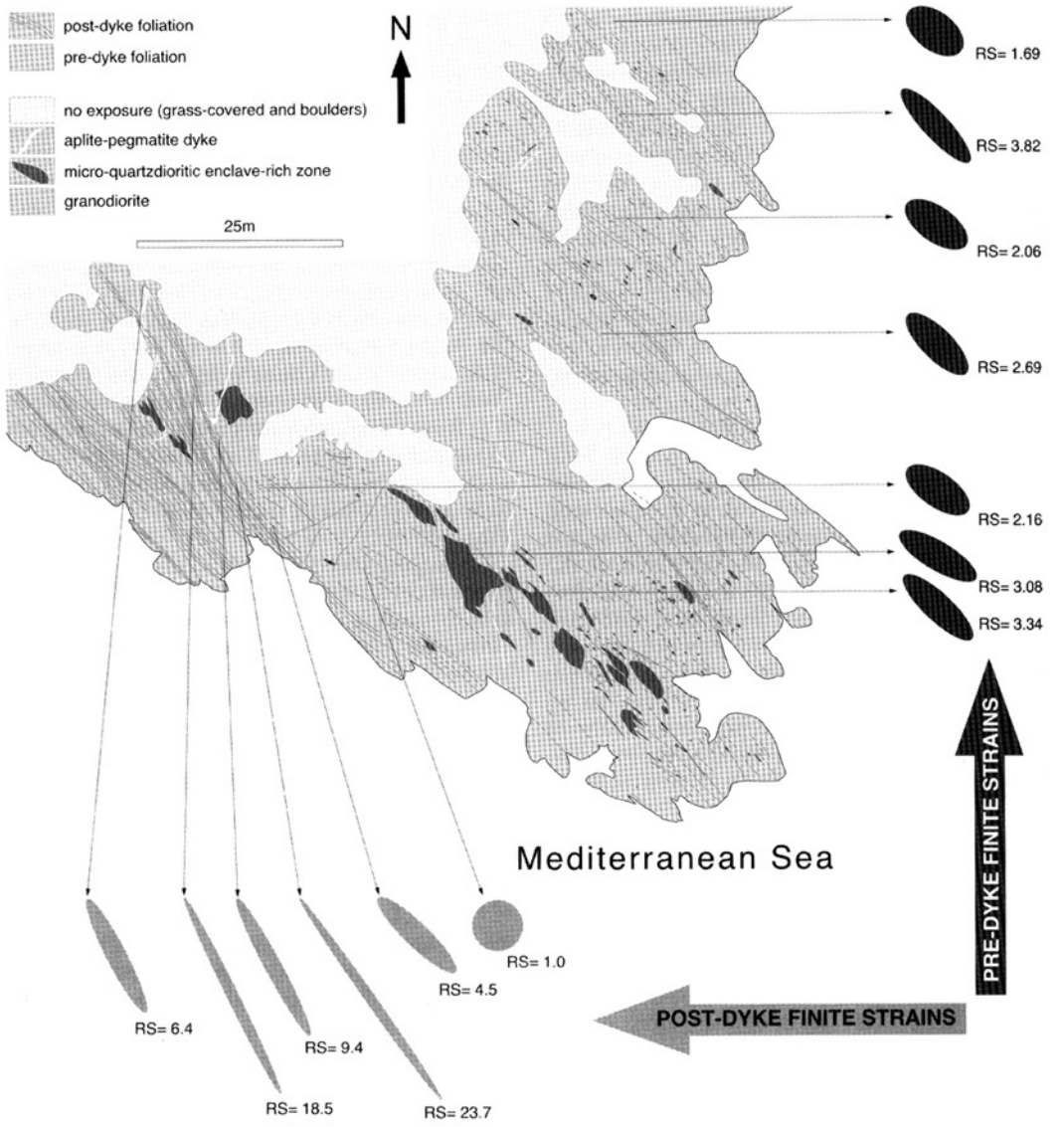

Fig. 7. Structural map and strain analysis of pre-dyke structures and post-dyke shear zones along a coastal section east of the Roses Lighthouse. In both cases strain analysis was performed using the Rf/ϕ technique for enclave populations. For each locality, the mean strain axial ratio (RS) is shown with an ellipse showing mean orientation and shape of the strain ellipse. Location is shown in Fig. 2.

deformation from the magmatic to the mylonitic stages, with the orientation of the regional shortening direction remaining fairly constant.

Furthermore, the preferred disposition of dykes, at high angle to the magmatic fabric, suggests that dyke emplacement occurred along tension fractures compatible with the strain field active during preceding and subsequent events. In this way, there is no need for an interkinematic regime or a shift in tectonic regime from compressional to extensional to explain dyke emplacement.

The structures observed in the Roses granodioritic stock developed during syntectonic cooling and reveal a continuity of deformation from high- to low-temperature conditions. A change of rheology from high- to low-temperature regime is capable of explaining the

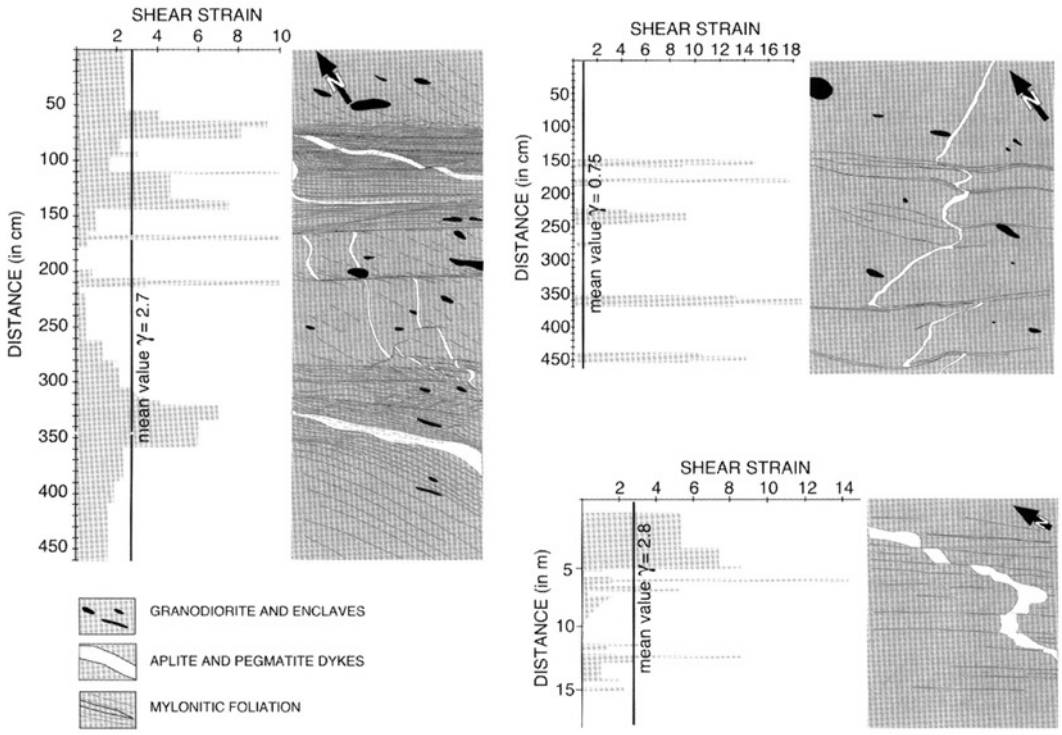

Fig. 8. Shear strain analysis across three sections in areas affected by inhomogeneous post-dyke shearing. Mean shear strain values have been calculated using total width versus total displacement relationships. All sections are plane-view.

observed structures and strain pattern. At high temperature, strain is distributed more homogeneously, whereas the progressive temperature drop induces a inhomogeneous strain pattern due to high strain localization along shear zones.

Two critical points in the rheological history of the stock can be identified:

(1) The first one took place at high temperature when the dykes intruded. At this stage, the granodioritic melt was close to completion of crystallization and probably below the critical fraction for magmatic flow. Thus, this first critical point would not be exactly contemporaneous with the 'rheologically critical melt percentage', theoretically and experimentally inferred as a sudden change of rocks strength caused by the crossing of a critical volume fraction of melt (Arzi 1978; Van der Molen & Paterson 1979; Dell' Angelo & Tullis 1988; Rutter & Neumann 1995; Vigneresse and Tikoff 1999). Most probably, high fluid pressures, induced by the presence of water saturated melts, favoured brittle tension fractures filled with the residual melts at this stage ('melt enhanced embrittlement'). Furthermore, a strain rate increase could also facilitate local brittle failure.

(2) The second critical point corresponds to the low temperature ductile–brittle transition in granitic rocks when shearing is replaced by discrete faults. Most of the overall deformation was accommodated during the ductile stages (magmatic fabric, high-temperature solid-state deformation and shear zones), whereas deformation accommodated during brittle stages was negligible relative to the total deformation.

Although no conclusive evidence for the strain regime responsible for synmagmatic deformation has been found in Roses, a dextral transpressional regime is inferred from correlation with the nearby northern Cap de Creus tectonometamorphic belt, where the kinematics are well established and documented (Carreras 2001; Druguet 2001). Moreover, this is also in accord with the work by Gleizes *et al.* (1998*b*) that indicates a dextral transpression as a main tectonic

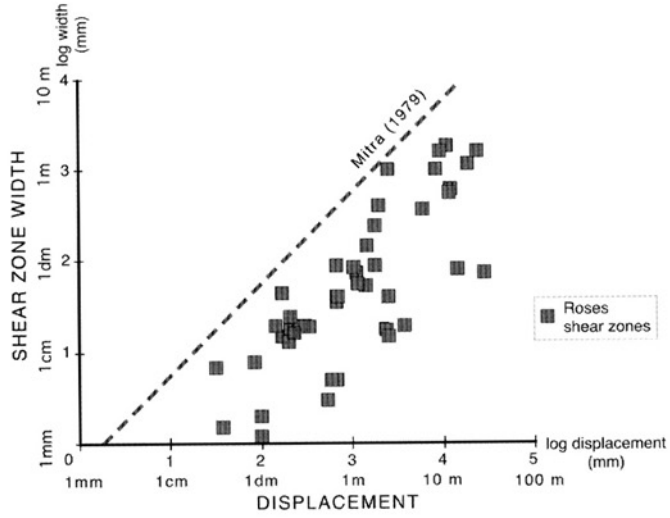

Fig. 9. Diagram of displacement against width measured in different sized shear zones. The displacement–width relationship line by Mitra (1979) has been drawn for comparison.

setting for the emplacement of granitoid batholiths in the Variscan of the Pyrenees.

This work was financed by the BTE2001-2616 project (M.C.Y.T). The manuscript has benefited greatly from thoughtful reviews by B. Miller and S. Johnson. We thank P. D. Bons for his kind comments and help with English. We also thank I. Tribe and C. Simpson for careful review and constructive comments on a previous version of the manuscript. The stereographic analysis was done with Stereonet, a program by R. W. Allmendinger.

References

ARZI, A. 1978. Critical phenomena in the rheology of partially melted rocks. *Tectonophysics*, **44**, 173–184.

BROWN, M. & SOLAR, G.S. 1998. Granite ascent and emplacement during contractional deformation convergent orogens. *Journal of Structural Geology*, **20**, 1365–1393.

CARRERAS, J. 2001. Zooming on Northern Cap de Creus shear zones. *Journal of Structural Geology*, **23**, 1457–1486

CARRERAS, J. & LOSANTOS, M. 1982. Geological setting of the Roses granodiorite, (E-Pyrenees, Spain). *Acta Geologica Hispanica*, **17**, 211–217.

CARRERAS, J., JULIVERT, M. & SANTANACH, P. 1980. Hercynian Mylonite Belts in the Eastern Pyrenees: an example of shear zones associated with late folding. *Journal of Structural Geology*, **2**, 5–9.

DAVIDSON, C., SCHMID, S.M. & HOLLISTER, L.S. 1994. Role of melt during deformation in the deep crust. *Terra Nova*, **7**, 133–142.

DELAPERRIÈRE, E., DE SAINT BLANQUAT, M., BRUNEL, M. & LANCELOT, J. 1994. Géochronoloige U–Pb sur zircons et monazites dans le massif du Saint Barthélemy (Pyrénées, France): discussion des âges des événements varisques et pré-varisques. *Bulletin de la Société Géologique de France*, **165**, 101–112.

DELL'ANGELO, L.N. & TULLIS, J. 1988. Experimental deformation of partially melted granitic aggregates. *Journal of Metamorphic Geology*, **6**, 495–515.

DRUGUET, E. 2001. Development of high thermal gradients by coeval transpression and magmatism during the Variscan orogeny: insights from the Cap de Creus (Eastern Pyrenees). *Tectonophysics*, **332**, 275–293.

EVANS, N.G., GLEIZES, G., LEBLANC, D. & BOUCHEZ, J.L. 1998. Syntectonic emplacement of the Maladeta granite (Pyrenees) deduced from relationships between Hercynian deformation and contact metamorphism. *Journal of the Geological Society, London*, **155**, 209–216.

GAPAIS, D. 1989. Shear structures within deformed granites: Mechanical and thermal indicators. *Geology*, **17**, 1144–1147.

GAY, N.C. 1968. Pure shear and simple shear deformation of inhomogeneous viscous fluid. 2. The determination of the total finite strain in rocks from objects such as deformed pebbles. *Tectonophysics*, **5**, 295–302.

GLEIZES, G., LEBLANC, D. & BOUCHEZ, J.L. 1991. Le pluton granitique de Bassiès (Pyrénées ariégoises): zonation, structure et mise en place. *Comptes Rendus de l'Académie des Sciences (Paris)*, **312**, 755–762.

GLEIZES, G., LEBLANC, D., SANTANA, V., OLIVIER, P. & BOUCHEZ, J.L. 1998*a*. Sigmoidal structures featuring dextral shear during emplacement of the Hercynian granite complex of Cauterets-Panticosa,

Pyrenees. *Journal of Structural Geology*, **20**, 1229–1245.

GLEIZES, G., LEBLANC, D. & BOUCHEZ, J.L. 1998*b*. The main phase of the Hercynian Pyrenees is a dextral transpression. *In*: HOLDSWORTH, R.E, STRACHAN, R.A & DEWEY, J.F. (eds) *Continental transpressional and transtensional tectonics*. Geological Society, London, Special Publications, **135**, 267–273.

GUITARD, G. 1970. Le métamorphisme hercynien mésozonal et les gneiss oeillés du massif du Canigou, (Pyrénées Orientales). *Mémoires du Bureau de Recherches Géologiques et Minières*, **63**, 353 pp.

HANDY, M.R., MULCH, A., ROSENAU, M. & ROSENBERG, C.L. 2001. The role of fault zones and melts as agents of weakening, hardening and differentiation of the continental crust: a synthesis. *In*: HOLDSWORTH, R.E., STRACHAN, R.A., MAGLOUGHLIN, J.F. & KNIPE, R.J. (eds) *The nature and tectonic significance of fault zone weakening*. Geological Society, London, Special Publications, **186**, 305–332.

HOLLISTER, L.S. & CRAWFORD, M.L. 1986. Melt-enhanced deformation: a major tectonic process. *Geology*, **14**, 558–561.

HUTTON, D.H.W. 1988. Granite emplacement mechanisms and tectonic controls: inferences from deformation studies. *Transactions of the Royal Society of Edinburgh*, **79**, 245–255.

LAMOUROUX, C., SOULA, J.C., DERAMOND, J. & DEBAT, P. 1980. Shear zones in the granodiorite massifs of the Central Pyrenees and the behaviour of these massifs during the Alpine orogenesis. *Journal of Structural Geology*, **2**, 49–53.

LEBLANC, D., GLEIZES, G., ROUX, L. & BOUCHEZ, J.L. 1996. Variscan dextral transpression in the French Pyrenees: new data from the Pic des Trois-Seigneurs granodiorite and its country rocks. *Tectonophysics*, **261**, 331–345.

LISLE, R.J. 1985. *Geological strain analysis: a manual for the Rf/ϕ technique*. Pergamon, Oxford.

MARRE, J. 1973. *Le complexe éruptif de Quérigut. Pétrologie, Structurologie, cinématique de mise en place*. Thèse Toulouse, 543 pp.

MITRA, G. 1979. Ductile deformation zones in Blue Ridge basement rocks and estimation of finite strains. *Geological Society of America Bulletin*, **90**, 935–951.

MUÑOZ, J.A., MARTÍNEZ, A. & VERGÉS, J. 1986. Thrust sequences in the Spanish eastern Pyrenees. *Journal of Structural Geology*, **8**, 399–405.

PATERSON, S.R. & MILLER, R.B. 1998. Stoped blocks in plutons: paleo-plumb bobs, viscometers, or chronometers? *Journal of Structural Geology*, **20**, 1261–1272.

PATERSON, S.R. & VERNON, R.H. 1995. Bursting the bubble of ballooning plutons: A return to nested diapirs emplaced by multiple processes. *Geological Society of America Bulletin*, **107**, 1356–1380.

PATERSON, S.R., VERNON, R.H. & TOBISCH, O.T. 1989. A review of criteria for the identification of magmatic and tectonic foliations in granitoids. *Journal of Structural Geology*, **11**, 349–363.

RAMSAY, J.G. & ALLISON, I. 1979. Structural analysis of shear zones in an Alpinised Hercynian granite. *Schweizerische Mineralogische und Petrographische Mitteilungen*, **59**, 251–279.

RAMSAY, J.G. & GRAHAM, R.D. 1970. Strain variations in shear belts. *Canadian Journal of Earth Sciences*, **7**, 786–813.

RAMSAY, J.G. & HUBBER, M.I. 1983. *The techniques of modern structural geology, Vol. 1: Strain analysis*. Academic Press, London.

RUTTER, E.H. & NEUMANN, D.H.K. 1995. Experimental deformation of partially molten westerly granite under fluid-absent conditions, with implications for the extraction of granitic magmas. *Journal of Geophysical Research*, **100** (B8), 15697–15715.

SAILLANT, J.P. 1982. *La faille de Mérens (Pyrénées Orientales) microstructures et mylonites*. Thèse 3ème cycle, 297 pp, Univ. Paris VII.

SIMPSON, C. 1983. Displacement and strain patterns from naturally occurring shear zone terminations. *Journal of Structural Geology*, **5**, 497–506.

SIMPSON, C., CARRERAS, J. & LOSANTOS, M. 1982. Inhomogeneous deformation in Roses granodiorite. *Acta Geologica Hispanica*, **17**, 219–226.

TOBISCH, O.T. & WILLIAMS, Q. 1998. Use of microgranitoid enclaves as solid state strain markers in deformed granitic rocks: an evaluation. *Journal of Structural Geology*, **20**, 727–743.

VAN DER MOLEN, I. & PATERSON, M.S. 1979. Experimental deformation of partially-melted granite. *Contributions to Mineralogy and Petrology*, **70**, 299–318.

VERGELY, P. 1970. *Etude tectonique des structures pyrénéenes du versant sud des Pyrénées orientales*. Thèse 3ème cycle, Faculté Sciences, Université de Montpellier.

VIGNERESSE, J.L. & TIKOFF, B. 1999. Strain partitioning during partial melting and crystallizing felsic magmas. *Tectonophysics*, **312**, 117–132.

WENK, H.R. 1998. Deformation of mylonites in Palm Canyon, California, based on xenolith geometry. *Journal of Structural Geology*, **20**, 559–571.

WILLIAMS, Q. & TOBISCH, O.T. 1994. Microgranitoid Enclaves shapes and magmatic strain histories: Constraints from drop deformation theory. *Journal of Geophysical Research*, **99**, 24359–24368.

ZWART, H.J. 1979. The geology of the central Pyrenees. *Leidse Geologische Mededelingen*, **50**, 1–74.